Properties of lipid electropores I: Molecular dynamics simulations of stabilized pores by constant charge imbalance☆

Maura Casciola [a,b,c], Marina A. Kasimova [a], Lea Rems [d], Sara Zullino [a,b], Francesca Apollonio [b], Mounir Tarek [a,e,*]

[a] Université de Lorraine, UMR 7565, F-54506 Vandoeuvre les Nancy, France
[b] Department of Information Engineering, Electronics and Telecommunications (D.I.E.T), Sapienza University of Rome, 00184 Rome, Italy
[c] Center for Life Nano Science@Sapienza, Istituto Italiano di Tecnologia, 00161 Rome, Italy
[d] University of Ljubljana, Faculty of Electrical Engineering, Tržaška 25, SI-1000 Ljubljana, Slovenia
[e] CNRS, UMR 7565, F-54506 Vandoeuvre les Nancy, France

ARTICLE INFO

ABSTRACT

Molecular dynamics (MD) simulations have become a powerful tool to study electroporation (EP) in atomic detail. In the last decade, numerous MD studies have been conducted to model the effect of pulsed electric fields on membranes, providing molecular models of the EP process of lipid bilayers. Here we extend these investigations by modeling for the first time conditions comparable to experiments using long (μs–ms) low intensity (~kV/cm) pulses, by studying the characteristics of pores formed in lipid bilayers maintained at a constant surface tension and subject to constant charge imbalance. This enables the evaluation of structural (size) and electrical (conductance) properties of the pores formed, providing information hardly accessible directly by experiments. Extensive simulations of EP of simple phosphatidylcholine bilayers in 1 M NaCl show that hydrophilic pores with stable radii (1–2.5 nm) form under transmembrane voltages between 420 and 630 mV, allowing for ionic conductance in the range of 6.4–29.5 nS. We discuss in particular these findings and characterize both convergence and size effects in the MD simulations. We further extend these studies in a follow-up paper (Rems et al., Bioelectrochemistry, Submitted), by proposing an improved continuum model of pore conductance consistent with the results from the MD simulations.

© 2016 Elsevier B.V. All rights reserved.

1. Introduction

Experimental evidence indicates that the application of an external electric field to biological cells affects transiently or permanently the integrity of their plasma membrane [1–8]. The changes in membrane integrity are manifested by a substantial increase in the membrane ionic conductance, an increase in molecular uptake into the cell and a release of the cytosolic content from the cell [9–13]. This effect has been rationalized by evidence demonstrating that an electrical pulse induces a large change in the transmembrane voltage resulting in rearrangements of the membrane components, in particular the lipid bilayer, leading to the formation of aqueous transmembrane pores [4–8, 14–16]. This process of 'aqueous pores' formation under the application of an external electric field is known as electroporation (EP) [1,12,17]. Today, EP is widely used in biomedicine and biotechnology for delivery of drugs or genetic material into cells [13,18–24].

The size of pores formed as a result of EP together with their morphology and conductive properties are crucial in determining the permeability and selectivity of the plasma membrane to different ionic and molecular species and consequently the potential efficacy of a given EP application. While extensive experimental work on cells and model lipid membranes (e.g. planar lipid bilayers and lipid vesicles) has been devoted to the structural characterization of these pores [25–35], the data emerging so far is very scarce. The nanometer-range size of the pores unfortunately limits the possibility of their direct observation by conventional techniques. Only very recently, time resolved visualization of pores in droplet interface bilayers was made possible using total internal reflection fluorescence microscopy [16]. Nevertheless, such fluorescence imaging currently does not allow the spatial resolution required to measure the pore size, nor the temporal resolution corresponding to conventional microsecond and millisecond pulses generally used in EP. Experimentally, therefore, one is able to estimate the nanopore dimension only indirectly by measuring either membrane permeability to molecules of different sizes, or membrane conductance recovered from the current/voltage relationship. Both approaches, however, have their specific limitations.

Estimates of pore size based on monitoring the transmembrane transport of small molecules (e.g. sugars, polyethylene glycols [33], bleomycin [34]) and fluorescent dyes (e.g. thallium ions [32], YO-PRO, propidium iodide [35]) were mostly obtained from in vitro experiments on cells after exposing them to nanosecond long (≤600 ns) electric

pulses. Results of these studies suggested that nanosecond pulses induce a high number of long-lived yet small pores, most of them with radii of about 0.5–0.7 nm, which allow the transport of larger molecules such as propidium iodide, but prevent the massive flux reported for longer (millisecond) less intense (kV/cm) pulses [35–38]. The direct correlation between the size of a molecule and that of a pore is though debatable for molecules that might interact strongly with the pore walls. Indeed an interacting molecule requires certain time to dissociate from the bilayer and diffuse into the cytosolic milieu where it can be detected. In addition, a charged molecule can significantly perturb the local electrostatic environment in the pore proximity, leading to changes in pore dimensions and pore morphology [39]. Even neutral sugar molecules can strongly interact with lipid headgroups through hydrogen bonding, consequently modifying the bilayer properties [40]. Such measurements may therefore not reflect properly the properties of pores as directly induced by electric pulses.

Estimates of pore size based on measurements of membrane conductance were on the other hand mostly obtained from planar lipid bilayers when applying a constant current (chronopotentiometry) to the membrane [25,26,29]. The benefit of controlling the current instead of the voltage is that once a pore is formed, the voltage across the membrane can reduce due to ionic transport through the pore, hence stabilizing the pore and preventing membrane rupture. For phosphatidylcholine based planar lipid bilayers, pore radii from 1.9 to 6.0 nm were reported, with larger pores observed when imposing a higher current. Conductance measurements have also been performed on dense cell suspensions during exposures to trains of 100 μs pulses [28] and on single cells using patch clamp techniques [30]. These studies suggested that pore radii can vary from ~1 to 55 nm, depending on the experimental conditions. However, the major limitation of estimating the pore size from conductance measurements is that the experimental data needs to be fitted to a certain model, which relates the pore conductance with the pore size. For such purpose, analytical models deriving from the continuum Nernst–Planck theory are normally used, which inherently impose simplified assumptions about the pore geometry and the effective conductivity of the electrolyte inside the pore [41–43]. The choice of such parameters and characteristics are in general arbitrary or too approximate, which may cast doubts on the accuracy of the predictions arising from the models. Moreover, continuum theories can fail to properly describe the physics in a molecular-scale system, which was indeed observed for ion channels [44,45]. One way of testing, validating, and if needed improving the continuum models is to compare them with molecular dynamics (MD) simulations, which provide full atomistic details of the entire process of ionic conduction through a pore.

This is precisely the approach we are undertaking hereafter. In a series of papers, we pursue a line of research where we use MD simulations to determine the structural (shape, size) and electrical (conductance, selectivity) properties of electropores formed in a model lipid bilayer in its liquid crystal L_α phase, when subject to increased transmembrane (TM) voltage. In the first (present) paper, we introduce a new MD simulation protocol that allows one to observe stable pores and extract their equilibrium properties under EP conditions. The results from the simulations are then further analyzed in our subsequent paper [46], where they are compared to the predictions of a continuum model constructed based on the model system in MD simulations. As we will demonstrate, improvement of the standard models is required in order to obtain results which are consistent with the molecular modeling.

In MD simulations, there are two common methods that allow the modeling of a TM voltage (trigger of EP): applying an external electric field and imposing a charge imbalance across a lipid bilayer. An external electric field is introduced into the system as an additional force acting on all the atoms charged [14,47–50]. In such a scheme, the reorientation of water molecules located at the solution/bilayer interface induces a TM voltage that, when overcoming a certain threshold, triggers EP. It was demonstrated, however, that in simulations with an external electric field, the pores keep expanding in their size while the field is

maintained above the EP threshold, indicating their instability [51]. Stabilization can be reached by lowering the intensity of the external electric field [52,53], but an arbitrary control of the field intensity hardly corresponds to a clear experiment.

In the charge imbalance method, a TM potential is generated by submitting lipid bilayers to ionic salt concentration gradients either considering two solution baths separated by two bilayers [54–56] (the double bilayer scheme) or by a bilayer and a vacuum slab [57] (the single bilayer scheme). In general, unlike the external electric field method, which rather mimics an experiment using high intensity nanosecond pulses [57,58], the charge imbalance method corresponds to the traditional EP setup where low microsecond/millisecond pulses are applied. Such a pulse applied to the membrane results indeed in the accumulation of charged species at both solution/membrane interfaces; if one considers the membrane as a capacitor embedded into conductive medium, a TM potential created by the accumulation of charges on this capacitor can be accordingly described.

The charge imbalance protocols used so far in simulations to model EP, suffer from two important shortcomings. First, the charge imbalance is not re-set during the simulation. Thus, in studies with the double [55, 56] and single bilayer [57,58] schemes, after the EP occurs, the imposed charge imbalance at the beginning decreases significantly within several tens/hundreds ps (depending on the system size) due to an exchange of ions through the pores in the bilayer. The decrease of the charge imbalance results in a TM voltage drop, which may ultimately lead to the pore collapse or resealing. A procedure to maintain the charge imbalance at a constant level was recently proposed by Kutzner *et al.* [59] to study the transport in ion channels. In this procedure, named "swapping", the number of ions in the two solution baths is frequently estimated and if the latter differs from the initial setup, a "swapping" event takes place: an ion of one solution is exchanged by a water molecule of the other solution bath.

The second shortcoming of the charge imbalance method as used so far in MD simulations concerns the membrane lateral expansion: the latter can hardly be controlled in the double bilayer scheme due to the fact that only one bilayer undergoes EP, and is prohibited in the single bilayer scheme because in this case the simulations are carried out at a constant volume. As a result, the pores are not allowed to relax to their equilibrium conformation and the quantitative estimation of their properties (*e.g.* size, current, selectivity to different ionic species, *etc.*) becomes unreliable.

In this work, we present a protocol that deals with both shortcomings of the charge imbalance method discussed so far. In particular, we used the "swapping" procedure [59] to maintain the charge imbalance at a constant level. Here, instead of considering the system with two bilayers, as used by Kutzner *et al.*, we adapted the procedure for the single bilayer scheme and the vacuum slab (see Fig. 1) proposed by our group [57]. In order to overcome the second shortcoming, which concerns the membrane lateral expansion, we used an assumption that in 'experimental' macroscopic systems (cells, liposomes or planar lipid bilayers) the formation of pores does not lead to any dramatic change in the membrane surface tension due to its dissipation. Hence we performed our simulations at a constant null surface tension. Using this protocol, we were able to model for the first time the EP process in conditions comparable with experiments. We show that in contrast to previous simulations [60–62], the pores relax to a stable conformation, which allows the estimation of their average size, ionic current and selectivity.

2. Methods

2.1. Systems preparation

Two systems with a hydrated Palmitoyl–Oleoyl–PhosphatidylCholine (POPC) bilayer were considered: a small one, composed by 256 POPC molecules (POPC_256), with a total size of $8.9 \times 8.9 \times 19$ nm³, and a big one, composed by 1024 POPC molecules (POPC_1024), with
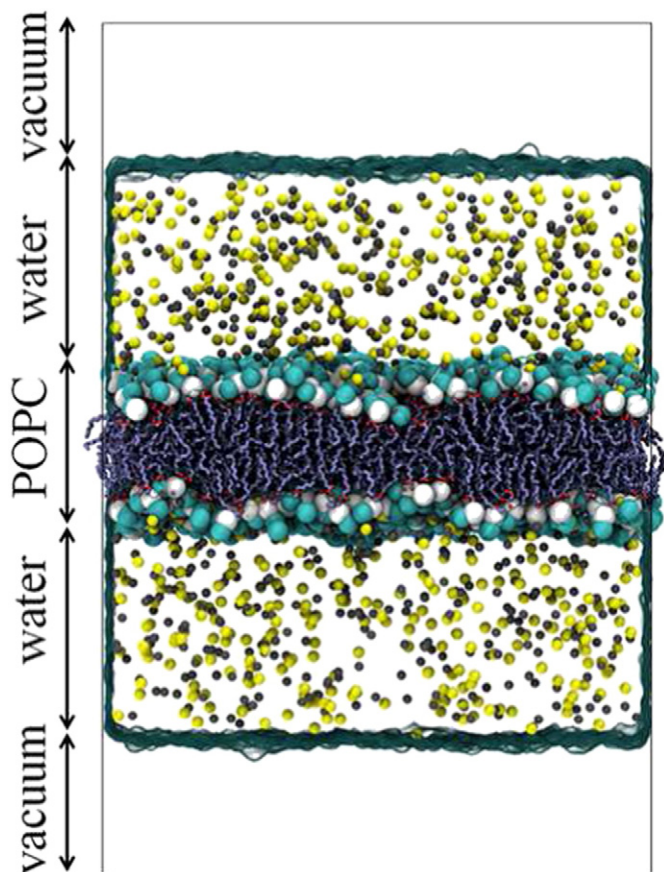
Fig. 1. The single bilayer scheme used in this work: two solution baths are separated by a lipid bilayer (POPC) and a vacuum slab, which prevent an exchange of ions and, hence, collapse of the charge imbalance. The POPC headgroups are shown as cyan and white beads, the tails are shown as purple sticks; sodium and chloride ions are colored in yellow and gray; water is transparent.

a total size of $17.8 \times 17.8 \times 19$ nm³. In both systems, the bilayers were surrounded by 1 M NaCl solution. The CHARMM36 force field [63] was used for POPC, and the TIP3P model was considered for water [64].

2.2. Parameters of MD

The MD simulations were performed using Gromacs 4.6. [65]. The equations of motion were integrated using the leap-frog algorithm, with a time step of 2.0 fs. The long-range electrostatic was calculated using Particle Mesh Ewald (PME). The cut-off distance of the short-range electrostatic was taken to be 1.2 nm. A switching function was used between 0.8 and 1.2 nm to smoothly bring the van der Waals forces and energies to 0 at 1.2 nm. During the simulations, chemical bonds between hydrogen and heavy atoms were constrained to their equilibrium values using LINCS. Periodic boundary conditions were applied in all directions.

2.3. Equilibration

The POPC_256 system was equilibrated during 100 ns in the NPT ensemble: pressure and temperature of the system were kept constant at 1 atm (using the Parrinello–Rahman barostat) and 300 K (using the Nose-Hoover thermostat), respectively. Note that at the temperature set for the study, the POPC bilayer is in its biologically relevant liquid crystal L_α phase. To verify the convergence of the equilibration we estimated the area per lipid along the run. The latter rapidly reached the plateau of ~61.8 Å², which is in agreement with the previously reported data for bare POPC bilayers [66].

The big system (POPC_1024) was further constructed by replicating the equilibrated POPC_256 in the bilayer plane. The POPC_1024 was additionally equilibrated during 20 ns.

Once the system is equilibrated, in order to impose a charge imbalance that induces a given TM voltage across the bilayer, the simulation box is extended in the direction perpendicular to the lipid plane (z) creating a vacuum slab. This procedure was introduced by Delemotte et al. [57,58] to reduce the computational costs of double layer schemes. In this series of papers, the authors demonstrated that, as far as the water baths surrounding the lipid bilayer are thicker than 2.5–3 nm, the presence of water/vacuum interfaces does not affect the bilayer properties.

2.4. Estimation of the total surface tension

During the equilibration performed in the NPT ensemble the total surface tension (γ/mN/m) in the system was zero since the lateral and the normal pressure to the solution/bilayer interface are set equal. However, in our further simulations we considered the scheme with a vacuum slab [57,58], which introduces an additional solution/vacuum interface with a non-zero surface tension. In the system with a vacuum slab, the total surface tension (γ_{tot}/mN/m) is the sum of the surface tension at the solution/bilayer ($\gamma_{sol/bilayer}$/mN/m) and solution/vacuum interfaces ($\gamma_{vacuum/sol}$/mN/m): $\gamma_{tot} = 2\gamma_{vacuum/sol} + \gamma_{bilayer/sol}$. Thus, in order to maintain throughout the simulations $\gamma_{bilayer/sol} \sim 0$ mN/m, one needs to constrain the total surface tension of the system to that of the vacuum/solution interface: $\gamma_{tot} = 2\gamma_{vacuum/sol}$.

In order to estimate the total surface tension, arising from the solution/vacuum interfaces we fixed its volume and performed short MD simulations (10 ns). Based on the obtained trajectories, a surface tension of ~100 mN/m was obtained from the lateral (P_l/bar) and the normal pressure to the solution/bilayer interface (P_t/bar) as: $\gamma = \int [P_l - P_t] dz$, i.e. the surface tension at each of the two vacuum/solution interfaces was ~50 mN/m, in agreement with the experimental measurements and modeling using similar force fields [67,68].

Notice that we used this value of surface tension for the two systems; POPC_256 and POPC_1024, testing its validity by looking at the evolution of the area of the simulation box in time. The latter remains constant over the elapsed time (see Fig. 6 of the Supplementary Material) both when the systems are at rest (no charge imbalance applied) and for low values of TM voltages when the membrane is porated. For higher values of TM voltage we register fluctuations of the box area due to the osmotic pressure induced by the ion and water flux through the pore (see Subsections 2.7 and 3.1).

2.5. Transmembrane (TM) potential

The electrostatic potential U_z/V along the normal to the bilayer can be calculated by solving Poisson's Eq. (1), i.e. derived as double integral of ρ_z/(C/m³), the volume charge density distribution, being ε_0/(F/m) the vacuum permittivity:

$$U_z = U(z) - U_0 = -\frac{1}{\varepsilon_0} \int_0^z \int_0^{z'} \rho_z\left(z''\right) dz'' dz'. \tag{1}$$

As reference, U_0 was set to zero in the lower bulk solution. Practically, we calculated the electrostatic potential after the pore formation (see Subsection 2.7) by dividing the system into 0.1 nm slices along Z-axis, summing the charges in each slice and integrating the resulting charge distribution for 10,000 configurations spread out over 20 ns time-windows. The TM voltage U_m/V was calculated as the difference between the electrostatic potential measured at the lower and the upper baths.

2.6. Swapping protocol

In order to maintain the applied charge imbalance $\Delta Q/C$ at a constant value, we used the "swapping" protocol [59] implemented in Gromacs. Briefly, the protocol works the following way: the program estimates the number of ions in the two solution baths and if this number differs from the initial setup, an ion of one solution bath is exchanged by a water molecule of the other solution bath. Here, we adapted the "swapping" protocol for the single bilayer scheme considering the Z-planes separating the two solution baths as the Z-coordinates of the water molecule center of mass placed in vacuum, and of the center of mass of the bilayer. The centers of mass of both groups were restrained during the simulations. Notice that no restraints are applied to the ions, which are free to flow and to contribute to the ionic current.

2.7. Production runs

The production runs of 100 ns each were performed in the NPγT ensemble (constant surface tension) using the single-bilayer scheme [57,58] and the "swapping" protocol [59]. In order to keep the total surface tension of the membrane/water at zero, we considered 100 mN/m as a reference value for the total surface tension γ_{tot} (see Subsection 2.4). To avoid the collapse of the vacuum slab, using the Berendsen barostat, we changed the compressibility of the system in the Z-direction (perpendicular to the bilayer) to zero, fixing the L_z-size of the box during the simulation.

For the POPC_256 the following $\Delta Q/C$ were applied: $0q_e$, $12q_e$ and $14q_e$ (q_e/C is the elementary charge). For the POPC_1024 in order to save computer time, we first porated the bilayer with a high charge imbalance ($90q_e$) to obtain pore formation in few ns. Once the pore was large enough (arbitrary value of 1.8 nm) four ΔQ were applied: $20q_e$, $32q_e$, $40q_e$, $56q_e$ corresponding to the TM voltages U_m of ~420, 510, 520 and 630 mV, respectively. Consequently, the TM voltages were estimated only after the pore formation.

Notice that the $48q_e$ ΔQ was considered only in our subsequent paper [46] to increase the statistic needed for a more detailed analysis of the pore conductance, carried out over time windows of 20 ns each. In fact, when the ΔQ is too high the bilayer shows a less stable behavior in time in terms of membrane area (see Supplementary Material). This is probably due to the osmotic pressure imposed by the water flow (see Subsection 3.1) that results in non-equal volumes of water in the two baths of the bilayer as well as in a corresponding increase in the ionic concentration where the water volume is reduced. Therefore, like in the case of $48q_e$, if such not predictable behavior was observed before 80 ns, the simulation was rejected. The $56q_e$ run exhibits this behavior after 80 ns, which allowed us to carry out the analysis until that.

2.8. Analysis of the pore

Based on the obtained trajectories, the minimum pore radius (R/nm), ionic current (I/nA), conductance (G/nS) and selectivity (S) were analyzed. The pore radius was estimated using HOLE [69] at each 250 ps. The program HOLE was designed to determine protein channel dimensions along the axis perpendicular to the bilayer, defining the radius in a given position as the largest possible sphere which can fit the channel without overlapping with van der Waals radii of any atomic species previously set. To adapt the algorithm to our case, we chose as reference atoms the phosphorous and nitrogen of the lipid headgroups considering configurations of the pore along the trajectory.

The ionic current was evaluated as the slope of the ionic flux at each 0.2 ps; the conductance was estimated as the ratio between the average ionic current and the TM potential applied.

In order to verify the convergence, the cumulative values of the pore radius and ionic current were calculated along the MD runs. The simulations were assumed to converge when the cumulative values reached their plateau values. Accordingly, the average values and their standard deviations were estimated for the plateau regions. The bilayer density (d/a.u.), thickness (t_m/nm) and an average molecular order parameter (P_{CH}) were extracted using the protocol suggested by Castillo *et al.* [70].

3. Results and discussion

Experimentally, when macroscopic systems are exposed to an electric pulse causing EP, the formation of the pores does not lead to dramatic changes in the membrane surface tension, as it is re-distributed along the entire membrane surface. Hence, if one wishes to model the EP process in conditions comparable with the experimental ones, the membrane surface tension should be kept constant (and null). In the single bilayer charge imbalance scheme that we considered in this work, the total surface tension is the sum of the surface tension at the bilayer/solution and the surface tension at the solution/vacuum interfaces (see Subsection 2.4). While the total surface tension is constant when the bilayer is intact, it rises abruptly after the pore formation occurs [14,71]. To avoid such unrealistic increase, we estimated the total surface tension during the equilibration step (no charge imbalance) and used this value to maintain the surface tension constant when the system was exposed to the charge imbalance (see Subsection 2.4). In order to prevent the collapse of the vacuum slab, we maintained the compressibility of the system in the Z-direction (perpendicular to the bilayer) to zero (see Subsection 2.7). Finally, the simulations were performed using the "swapping" procedure proposed by Kutzner *et al.* [59] which allows to maintain the charge imbalance constant (see Subsection 2.6).

The protocol that combines the constant surface tension and constant charge imbalance was applied to the big system with 1024 POPC molecules (POPC_1024, see Subsection 2.1). Four different ΔQ were considered ($20q_e$, $32q_e$, $40q_e$, $56q_e$), corresponding to TM voltages U_m of ~420, 510, 520 and 630 mV, respectively (estimated after the bilayer electroporation, Fig. 2, as explained in Subsection 2.7).

In the following sections we report a detailed analysis of the pore radius, current, conductance and selectivity (Section 3.1) and of the
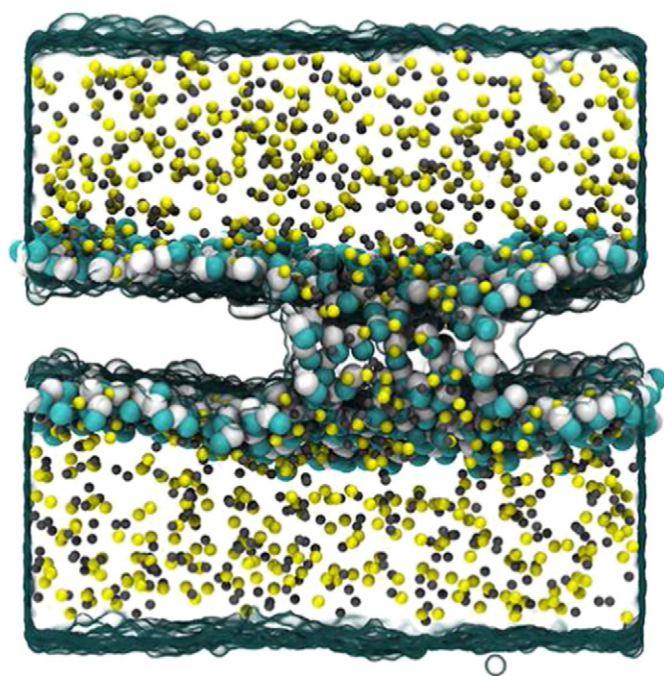

Fig. 2. Cross section of an electroporated POPC_1024 bilayer depicted from a configuration with a pore radius of 1.8 nm. The POPC headgroups are shown as cyan and white beads, the tails are transparent; sodium and chloride ions are colored in yellow and gray; water is transparent.

size effect induced by the finite dimension of the simulation cell (Section 3.2) obtained under the aforesaid described conditions.

3.1. Pore characteristics

Fig. 3 reports the cumulative average of the pore radius along the MD run and the average pore profile estimated for the four charge imbalances. The cumulative pore radii (Fig. 3A) reach a plateau after 20 ns indicating that the pores are stable and that the corresponding simulations have converged. For each MD run, the average pore radius and the standard deviation were further estimated for the remaining part of the trajectory: from 20 to 80 ns. In the Supplementary Material, Fig. 4, we report the time-averaged analysis on the pore radius and its standard deviation over segments of 20 ns as estimation of the fluctuations. Note that for the lowest value of ΔQ ($20q_e$), after the first 20 ns of simulation the time average of the minimum radius converges to a mean value around 1 nm with standard deviations overlapping (Fig. 4A of the Supplementary Material). Hence, for the scope of this paper, we consider the radius stable enough to test our protocol under ΔQ.

The average pore radius (Fig. 3B), ranging from 1 to 2.5 nm, was shown to be dependent on the charge imbalance applied to the system, thereby being dependent also on the TM voltage; the dependence of the average pore radius on the TM voltage is approximately linear in the investigated range.

Our observation of stable pores at moderate TM voltages is in general agreement with theoretical predictions [6,72–74]. The theory of EP namely predicts that once the energetic barrier for pore formation is overcome, the formed hydrophilic pore will stabilize at certain radius which corresponds to the local minimum in the pore free energy landscape. The position of this minimum with respect to the pore radius is also expected to shift with increasing TM voltage, resulting in larger stable pores. If the TM voltage exceeds a certain value, however, the minimum is expected to disappear leading to irreversible expansion of the pore and ultimate rupture of the bilayer provided that the TM voltage remains constant. We interpret our results as being in the range of TM voltages which allow pores to remain stable, at least in the time window considered.

The ionic current through the pore was estimated as the slope of the ionic flux (see Supplementary Material). In Fig. 4A we report the cumulative average of the ionic current for the four charge imbalances over time. As expected, the currents grow to reach a plateau after less than 10 ns until the end of the runs, which proves the convergence of this observable. The stable currents range from 2.69 to 18.58 nA, when the TM voltages from 420 to 630 mV are maintained.

The current/voltage relationship of Fig. 4B shows that as the TM voltage applied is increased, the current flowing through the single electropore rises approximately linearly. Note that with increasing

TM voltage the pore radius also increases. Since pores with larger size allow the passage of a higher number of ions, the increase in the current is both due to the increase in the TM voltage by directly increasing the electrophoretic drift of ions, as well as the increase in the pore size.

The conductance (G/nS) of the pore was calculated as the ratio of ionic current (I/nA) and TM voltage (U_m/V); the results are presented in Fig. 5A. We reported G as a function of the pore radius (R/nm) to facilitate the correlation of our results with the experimental ones, where the radius is indirectly deduced from the conductance measured. In the range of TM potentials investigated, the conductance changes almost linearly with the pore radius (for further analyses and discussions on the relationship between the pore conductance, pore shape, and pore radius we refer the reader to our subsequent paper [46]).

Finally, we estimated the pore selectivity (S) as the ratio of anionic (I_{Cl^-}/nA) to cationic (I_{Na^+}/nA) current, Fig. 5B. In agreement with the previous findings [53], the pore was shown to be more selective to sodium ions than to chloride ions. Ho et al. [53] extensively analyzed and discussed the effects of the pore wall and the interactions among the ions passing through nanoscale pores on the conductance, coming to the conclusion that this selectivity arises from the nature of the lipid molecules constituting the pore. The negatively charged phosphate groups that form the walls of the pore attract sodium ions, which hinders their passage across the bilayer, also makes the pore interior electrostatically unfavorable for cations.

As in the case of flat bilayers, the Na cations bind deeply and therefore for longer time scale that their Cl anionic counterpart. Consequently, as we show in Fig. 5B, the ratio of Cl and Na current decreases as the pore expands. Indeed, the pore expansion results in a higher fraction of those sodium ions that pass the pore without any hindrance as they do not interact with the pore walls. According to the analysis we performed in our subsequent paper [46], the pore selectivity to Cl ions can partially arise also due to electroosmotic flux of water through the pore, which enhances the current of Cl ions and at the same time reduces the current of Na ions. Indeed, in all performed simulations, we observed a net flux of water in the direction of the flux of Cl ions (i.e., opposite to the direction of the electric potential gradient), which can be attributed to the interactions of water with electrophoretically driven charged ions. The water flux gradually reduces the volume of water on one side of the bilayer and increases the volume of water on the other side. The changes in water volume limit the time range for which the simulations can be performed (~100 ns) in the absence of excessive osmotic pressure, which can lead to instability of the simulated system.

In a similar study carried out by Gurtovenko et al. [75] strong interactions of Na ions with lipid headgroups were witnessed, with a consequent slowdown of their permeation through hydrophilic water pores. However, the Na and Cl ions are found to cross the pore at nearly the
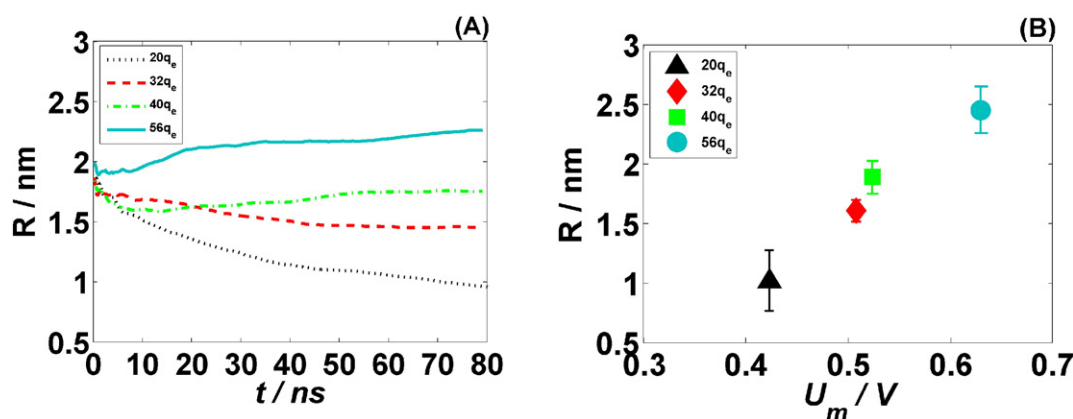

Fig. 3. (A) Cumulative minimum pore radius R/nm along the elapsed time t/ns, corresponding to the charge imbalances ΔQ/C of $20q_e$ (black dotted line), $32q_e$ (red dashed line), $40q_e$ (green dot-dashed line) and $56q_e$ (cyan solid). (B) Minimum pore radius R/nm versus the TM voltage U_m established at charge imbalances ΔQ/C of $20q_e$ (black triangle), $32q_e$ (red diamond), $40q_e$ (green square) and $56q_e$ (cyan circle).
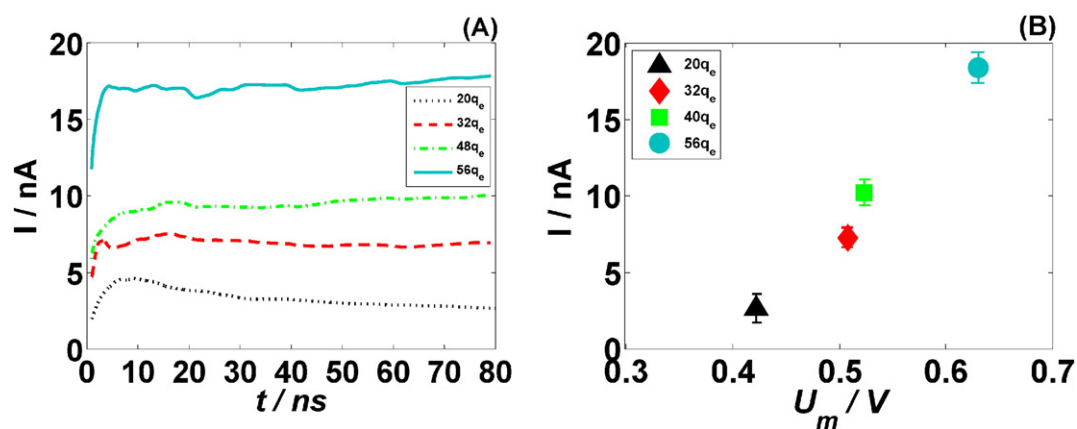
Fig. 4. (A) Cumulative average of the ionic current I/nA along the elapsed time t/ns, corresponding to the charge imbalances ΔQ/C of $20q_e$ (black dotted line), $32q_e$ (red dashed line), $40q_e$ (green dot-dashed line) and $56q_e$ (cyan solid line). (B) Current/voltage relationship for the charge imbalances ΔQ/C of $20q_e$ (black triangle), $32q_e$ (red diamond), $40q_e$ (green square) and $56q_e$ (cyan circle).

same ratio. It is worth to notice that in these set of simulations the charge imbalance was not maintained, and therefore after the leak of one ion the potential drops and the pore tends to collapse. Moreover, in such case the water flux that enhances the Cl flux is missing. This condition of instability could influence the transport of ions and the result reported from [75] can be considered only a qualitative indication.

In other studies such as those by Dzubiella et al. [76,77], such selectivity was also observed for transport in hydrophobic pores.

3.2. Simulation cell and size effects

In MD simulations, the EP of bilayers is commonly studied on relatively small systems composed of 256, 128 and in some cases of 64 lipids. Accordingly, we compared our data discussed so far (1024 lipids and a total size at rest of $17.8 \times 17.8 \times 19$ nm^3) with a smaller system of dimensions at rest $8.9 \times 8.9 \times 19$ nm^3, containing 256 POPC molecules (see Subsection 2.1); the results of the comparison are presented in Table 1. We found that at similar TM voltages the pore radius in the POPC_256 bilayer is almost twice lower than that in the POPC_1024 bilayer, which results as well in different values of conductance. We hypothesize that the observed inconsistency of the results stems from the size effect. Indeed, once a pore is formed in the POPC_256, the size of the simulation box prevents its adequate expansion, i.e. the bilayer patch is not large enough to allow for the release of tension induced by the pore spanning which consequently induces a constraint on the pore size.

In order to test this hypothesis, we analyzed the density, thickness and order parameters of the electroporated POPC_1024 and POPC_256 bilayers (Fig. 6). The lipid order parameter, defined as $P_{CH} = 1/2 <3\cos^2 \theta - 1>$, where θ is the angle between the C—H bond vector and the membrane normal, was calculated for all carbons in the lipid acyl chains and then averaged within each voxel over the ensemble of lipids and over the simulation (see Subsection 2.8).

The presence of the pore locally changes the bilayer properties; the headgroups surrounding the pore slide along the water column to stabilize it, resulting in a toroidal shape, and causing: a decrease in the order parameter, a local drop in the lipid density, and in the bilayer thickness. Fig. 6A and 6E show clearly that for the small system, the pore is too large with respect to the cell size. The area affected by the pore (where we register a decrease in the value of the properties mentioned above) almost reaches the patch borders, which probably influences through the periodic boundary condition its own stability and expansion. On the contrary, in the POPC_1024 the values of the density (d/a.u.) and the average molecular order parameter (P_{CH}) (Fig. 6B and 6F respectively) recover when moving away from the water defect.

4. Conclusions

Here we introduced a new protocol that enables for the first time to perform MD simulations of electroporated bilayer under conditions similar to those of experiments using low intensity, long (μs–ms) pulses. This is perceived as the most appropriate approach to directly determine the transport of ions and selected molecules across bilayers
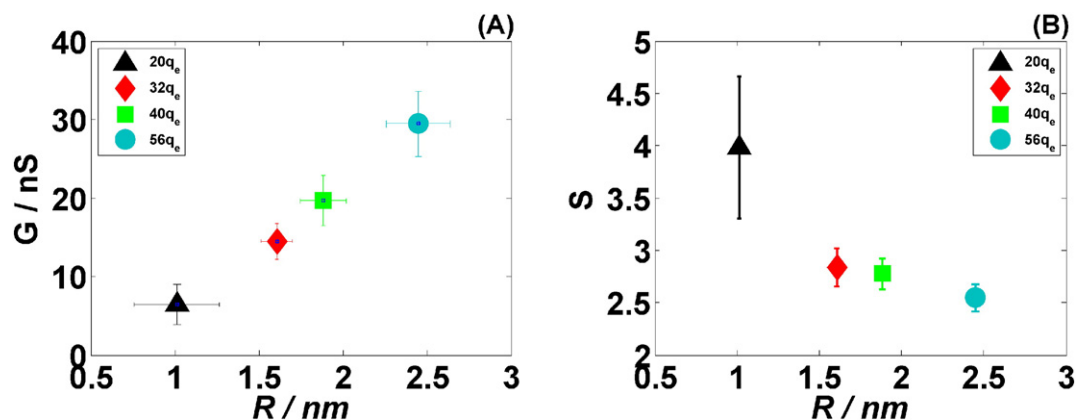

Fig. 5. Ionic conductance G/nS (A) and ionic selectivity S (B) as a function of the minimum pore radius R/nm, corresponding to the charge imbalances ΔQ/C of $20q_e$ (black triangle), $32q_e$ (red diamond), $40q_e$ (green square) and $56q_e$ (cyan circle).

Table 1
Pore radius R/nm and conductance G/nS estimated at specific TM potentials U_m/V.

System	$\Delta Q/q_e$	U_m/V	R/nm	G/nS
POPC_1024	20	0.42 ± 0.04	1.0 ± 0.3	6.4 ± 2.5
	40	0.52 ± 0.05	1.9 ± 0.2	19.6 ± 3.2
POPC_256	12	0.46 ± 0.06	0.6 ± 0.1	2.3 ± 0.2
	14	0.54 ± 0.10	0.7 ± 0.2	2.8 ± 1.2

ΔQ — charge imbalance imposed.
U_m — transmembrane potential create by the charge imbalance ΔQ.
R — minimum pore radius maintained by a given U_m.
G — conductance of the elctropore for the corresponding radius.

exposed to electric pulses, which remains a challenge for experimental methods. We proposed the use of an ensemble that allows the membrane surface tension γ_{tot} to be constant, avoiding unrealistic constrains. Then, the establishment of a constant voltage comparable with experimental exposures was guaranteed by the swap procedure. Both these conditions permit the formation of relaxed stable pores that can be characterized geometrically and electrically. The cumulative average of the pore radius and that of the ionic current confirm indeed the convergence of these observables after 20 ns of simulation run.

We found that for TM voltages ranging from 420 mV to 630 mV, the pore radius increases from 1 to 2.5 nm and the conductance from 6.4 to 29.5 nS. Quite interestingly, when the same TM voltage was maintained on the lipid patch of the sizes usually employed in MD simulations ($\sim 8.8 \times 8.8$ nm^2, 256 lipids) the pore radius obtained was twice smaller and the conductance almost three times smaller than what we reported for the large system ($\sim 17.8 \times 17.8$ nm^2, 1024 lipids), likely a consequence of the constrains imposed by the finite size of the simulation box.

Simulations along these lines should contribute to a better understanding of phenomenon of electroporation. Two further applications can be considered. First, investigating the EP of more complex membranes, and second investigating the transport of large molecules, *e.g.* drugs and genetic material to shed light on the uptake mechanisms.

To provide a further insight to the EP process these results need also to be linked with experimental observations. Since the direct comparison is challenging, as stated in the Introduction section, an intermediate and complementary step could be the use of continuum models. In the following paper, we therefore constructed a numerical model of pore conductance based on the Poisson–Nernst–Planck theory, and found a surprisingly exquisite agreement between the two approaches.

Acknowledgements

Appendix A. Supplementary data

Supplementary data to this article can be found online at http://dx.doi.org/10.1016/j.bioelechem.2016.01.006.

References

[1] E. Neumann, A.E. Sowers, C.A. Jordan, Electroporation and Electrofusion in Cell Biology, Springer Science & Business Media, 1989.
[2] J.A. Nickoloff, Animal Cell Electroporation and Electrofusion Protocols, Humana Press, NJ, 1995.
[3] S. Li, Electroporation Protocols : Preclinical and Clinical Gene Medicine, Humana Press, Totowa, N.J., 2008
[4] I.G. Abidor, V.B. Arakelyan, L.V. Chernomordik, Y.A. Chizmadzhev, V.F. Pastushenko, M.P. Tarasevich, Electric breakdown of bilayer lipid membranes: I. The main experimental facts and their qualitative discussion, J. Electroanal. Chem. Interfacial Electrochem. 104 (1979) 37–52, http://dx.doi.org/10.1016/S0022-0728(79)81006-2.
[5] R. Benz, F. Beckers, U. Zimmermann, Reversible electrical breakdown of lipid bilayer membranes: a charge-pulse relaxation study, J. Membr. Biol. 48 (1979) 181–204, http://dx.doi.org/10.1007/BF01872858.
[6] J.C. Weaver, Y.A. Chizmadzhev, Theory of electroporation: a review, Bioelectrochem. Bioenerg. 41 (1996) 135–160, http://dx.doi.org/10.1016/S0302-4598(96)05062-3.
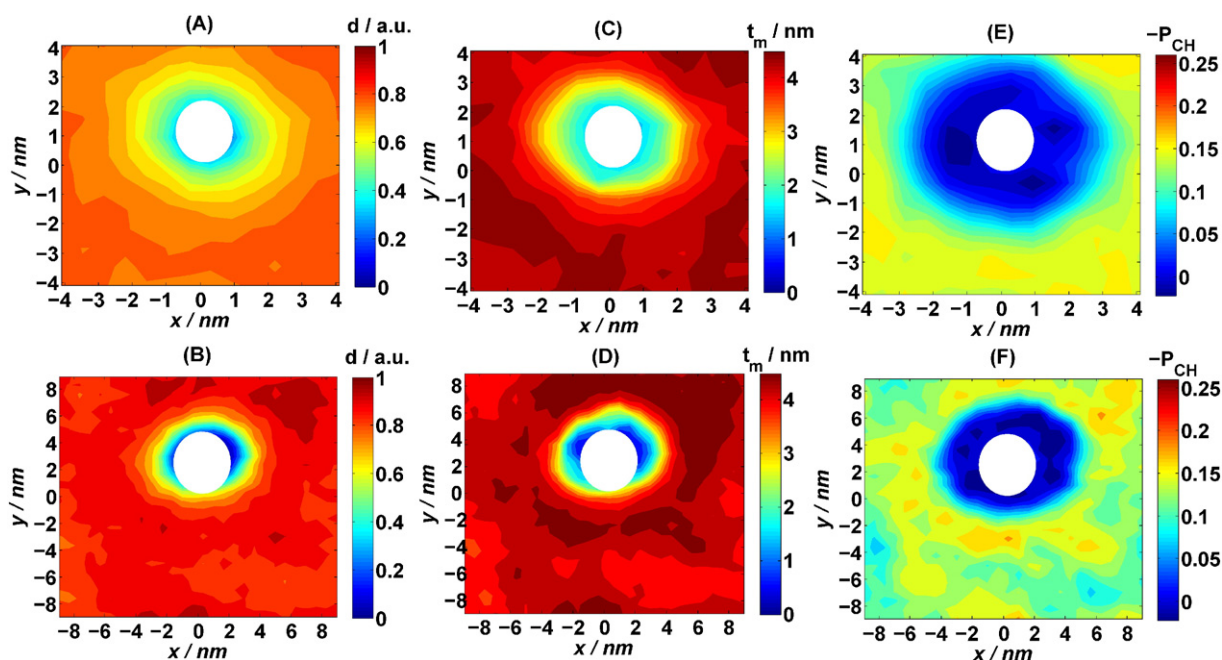[7] J.C. Weaver, Electroporation of biological membranes from multicellular to nano scales, IEEE Trans. Dielectr. Electr. Insul. 10 (2003) 754–768, http://dx.doi.org/10.1109/TDEI.2003.1237325.

Fig. 6. 2D spatial maps of the density d/a.u (A and B), thickness t_m/nm (C and D) and order parameter P_{CH} (E and F) estimated for the POPC_256 (A, C, E) and POPC_1024 (B, D, F) bilayers subject to 540 and 520 mV, respectively.

[8] C. Chen, S.W. Smye, M.P. Robinson, J.A. Evans, Membrane electroporation theories: a review, Med. Biol. Eng. Comput. 44 (2006) 5–14, http://dx.doi.org/10.1007/s11517-005-0020-2.

[9] G. Pucihar, T. Kotnik, D. Miklavcic, J. Teissié, Kinetics of transmembrane transport of small molecules into electropermeabilized cells, Biophys. J. 95 (2008) 2837–2848, http://dx.doi.org/10.1529/biophysj.108.135541.

[10] M. Hibino, M. Shigemori, H. Itoh, K. Nagayama, K. Kinosita, Membrane conductance of an electroporated cell analyzed by submicrosecond imaging of transmembrane potential, Biophys. J. 59 (1991) 209–220.

[11] M. Breton, L. Delemotte, A. Silve, L.M. Mir, M. Tarek, Transport of siRNA through lipid membranes driven by nanosecond electric pulses: an experimental and computational study, J. Am. Chem. Soc. 134 (2012) 13938–13941, http://dx.doi.org/10.1021/ja3052365.

[12] L.M. Mir, H. Banoun, C. Paoletti, Introduction of definite amounts of nonpermeant molecules into living cells after electropermeabilization: direct access to the cytosol, Exp. Cell Res. 175 (1988) 15–25.

[13] J. Teissié, N. Eynard, B. Gabriel, M.P. Rols, Electropermeabilization of cell membranes, Adv. Drug Deliv. Rev. 35 (1999) 3–19, http://dx.doi.org/10.1016/S0169-409X(98)00060-X.

[14] M. Tarek, Membrane electroporation: a molecular dynamics simulation, Biophys. J. 88 (2005) 4045–4053, http://dx.doi.org/10.1529/biophysj.104.050617.

[15] T. Kotnik, G. Pucihar, D. Miklavčič, Induced transmembrane voltage and its correlation with electroporation-mediated molecular transport, J. Membr. Biol. 236 (2010) 3–13, http://dx.doi.org/10.1007/s00232-010-9279-9.

[16] M. Szabo, M.I. Wallace, Imaging potassium-flux through individual electropores in droplet interface bilayers, Biochim. Biophys. Acta (2015) http://dx.doi.org/10.1016/j.bbamem.2015.07.009.

[17] T. Kotnik, P. Kramar, G. Pucihar, D. Miklavcic, M. Tarek, Cell membrane electroporation−part 1: the phenomenon, IEEE Electr. Insul. Mag. 28 (2012) 14–23, http://dx.doi.org/10.1109/MEI.2012.6268438.

[18] S. Lakshmanan, G.K. Gupta, P. Avci, R. Chandran, M. Sadasivam, A.E.S. Jorge, et al., Physical energy for drug delivery; poration, concentration and activation, Adv. Drug Deliv. Rev. 71 (2014) 98–114, http://dx.doi.org/10.1016/j.addr.2013.05.010.

[19] J. Villemejane, L.M. Mir, Physical methods of nucleic acid transfer: general concepts and applications, Br. J. Pharmacol. 157 (2009) 207–219, http://dx.doi.org/10.1111/j.1476-5381.2009.00032.x.

[20] J. Teissie, Electrically Mediated Gene Delivery: Basic and Translational Concepts, INTECH Open Access Publisher, 2013.

[21] M. Breton, L.M. Mir, Microsecond and nanosecond electric pulses in cancer treatments, Bioelectromagnetics 33 (2012) 106–123, http://dx.doi.org/10.1002/bem.20692.

[22] M.L. Yarmush, A. Golberg, G. Serša, T. Kotnik, D. Miklavčič, Electroporation-based technologies for medicine: principles, applications, and challenges, Annu. Rev. Biomed. Eng. 16 (1) (2014) 295.

[23] R. Cadossi, M. Ronchetti, M. Cadossi, Locally enhanced chemotherapy by electroporation: clinical experiences and perspective of use of electrochemotherapy, Future Oncol. 10 (2014) 877–890, http://dx.doi.org/10.2217/fon.13.235.

[24] D. Miklavčič, B. Mali, B. Kos, R. Heller, G. Serša, Electrochemotherapy: from the drawing board into medical practice, Biomed. Eng. Online 13 (2014) 29, http://dx.doi.org/10.1186/1475-925X-13-29.

[25] S. Kalinowski, G. Ibron, K. Bryl, Z. Figaszewski, Chronopotentiometric studies of electroporation of bilayer lipid membranes, Biochim. Biophys. Acta Biomembr. 1369 (1998) 204–212, http://dx.doi.org/10.1016/S0005-2736(97)00222-8.

[26] S. Koronkiewicz, S. Kalinowski, K. Bryl, Programmable chronopotentiometry as a tool for the study of electroporation and resealing of pores in bilayer lipid membranes, Biochim. Biophys. Acta 1561 (2002) 222–229.

[27] S. Koronkiewicz, S. Kalinowski, Influence of cholesterol on electroporation of bilayer lipid membranes: chronopotentiometric studies, Biochim. Biophys. Acta Biomembr. 1661 (2004) 196–203, http://dx.doi.org/10.1016/j.bbamem.2004.01.005.

[28] M. Pavlin, M. Kandušer, M. Reberšek, G. Pucihar, F.X. Hart, R. Magjarevic, et al., Effect of cell electroporation on the conductivity of a cell suspension, Biophys. J. 88 (2005) 4378–4390, http://dx.doi.org/10.1529/biophysj.104.048975.

[29] M. Kotulska, Natural fluctuations of an electropore show fractional Lévy stable motion, Biophys. J. 92 (2007) 2412–2421, http://dx.doi.org/10.1529/biophysj.106.091363.

[30] H. Krassen, U. Pliquett, E. Neumann, Nonlinear current–voltage relationship of the plasma membrane of single CHO cells, Bioelectrochemistry 70 (2007) 71–77, http://dx.doi.org/10.1016/j.bioelechem.2006.03.033.

[31] P. Kramar, L. Delemotte, A.M. Lebar, M. Kotulska, M. Tarek, D. Miklavčič, Molecular-level characterization of lipid membrane electroporation using linearly rising current, J. Membr. Biol. 245 (2012) 651–659, http://dx.doi.org/10.1007/s00232-012-9487-6.

[32] A.M. Bowman, O.M. Nesin, O.N. Pakhomova, A.G. Pakhomov, Analysis of plasma membrane integrity by fluorescent detection of Tl(+) uptake, J. Membr. Biol. 236 (2010) 15–26, http://dx.doi.org/10.1007/s00232-010-9269-y.

[33] O.M. Nesin, O.N. Pakhomova, S. Xiao, A.G. Pakhomov, Manipulation of cell volume and membrane pore comparison following single cell permeabilization with 60- and 600-ns electric pulses, Biochim. Biophys. Acta 1808 (2011) 792–801, http://dx.doi.org/10.1016/j.bbamem.2010.12.012.

[34] A. Silve, I. Leray, L.M. Mir, Demonstration of cell membrane permeabilization to medium-sized molecules caused by a single 10 ns electric pulse, Bioelectrochemistry 87 (2012) 260–264, http://dx.doi.org/10.1016/j.bioelechem.2011.10.002.

[35] A.G. Pakhomov, E. Gianulis, P.T. Vernier, I. Semenov, S. Xiao, O.N. Pakhomova, Multiple nanosecond electric pulses increase the number but not the size of long-lived nanopores in the cell membrane, Biochim. Biophys. Acta 1848 (2015) 958–966, http://dx.doi.org/10.1016/j.bbamem.2014.12.026.

[36] J. Deng, K.H. Schoenbach, E. Stephen Buescher, P.S. Hair, P.M. Fox, S.J. Beebe, The effects of intense submicrosecond electrical pulses on cells, Biophys. J. 84 (2003) 2709–2714, http://dx.doi.org/10.1016/S0006-3495(03)75076-0.

[37] P.T. Vernier, Y. Sun, L. Marcu, S. Salemi, C.M. Craft, M.A. Gundersen, Calcium bursts induced by nanosecond electric pulses, Biochem. Biophys. Res. Commun. 310 (2003) 286–295, http://dx.doi.org/10.1016/j.bbrc.2003.08.140.

[38] P.T. Vernier, Y. Sun, M.A. Gundersen, Nanoelectropulse-driven membrane perturbation and small molecule permeabilization, BMC Cell Biol. 7 (2006) 37, http://dx.doi.org/10.1186/1471-2121-7-37.

[39] F. Salomone, M. Breton, I. Leray, F. Cardarelli, C. Boccardi, D. Bonhenry, et al., High-yield nontoxic gene transfer through conjugation of the CM18-Tat11 chimeric peptide with nanosecond electric pulses, Mol. Pharm. 11 (2014) 2466–2474, http://dx.doi.org/10.1021/mp500223t.

[40] J. Kapla, J. Wohlert, B. Stevensson, O. Engström, G. Widmalm, A. Maliniak, Molecular dynamics simulations of membrane-sugar interactions, J. Phys. Chem. B 117 (2013) 6667–6673, http://dx.doi.org/10.1021/jp402385d.

[41] A. Barnett, The current–voltage relation of an aqueous pore in a lipid bilayer membrane, Biochim. Biophys. Acta Biomembr. 1025 (1990) 10–14, http://dx.doi.org/10.1016/0005-2736(90)90184-P.

[42] S. Kakorin, E. Neumann, Ionic conductivity of electroporated lipid bilayer membranes, Bioelectrochem. Amsterdam Neth. 56 (2002) 163–166.

[43] J. Li, H. Lin, The current–voltage relation for electropores with conductivity gradients, Biomicrofluidics 4 (2010) http://dx.doi.org/10.1063/1.3324847.

[44] G. Moy, B. Corry, S. Kuyucak, S.-H. Chung, Tests of continuum theories as models of ion channels. I. Poisson–Boltzmann theory versus Brownian dynamics, Biophys. J. 78 (2000) 2349–2363, http://dx.doi.org/10.1016/S0006-3495(00)76780-4.

[45] B. Corry, S. Kuyucak, S.-H. Chung, Tests of continuum theories as models of ion channels. II. Poisson–Nernst–Planck theory versus Brownian dynamics, Biophys. J. 78 (2000) 2364–2381, http://dx.doi.org/10.1016/S0006-3495(00)76781-6.

[46] L. Rems, M. Tarek, M. Casciola, D. Miklavcic, Properties of lipid electropores II: Comparison of continuum-level modeling of pore conductance to molecular dynamics simulations, Bioelectrochemistry, Unpublished results (Submitt. Rev.)

[47] D.P. Tieleman, The molecular basis of electroporation, BMC Biochem. 5 (2004) 10, http://dx.doi.org/10.1186/1471-2091-5-10.

[48] Q. Hu, S. Viswanadham, R. Joshi, K. Schoenbach, S. Beebe, P. Blackmore, Simulations of transient membrane behavior in cells subjected to a high-intensity ultrashort electric pulse, Phys. Rev. E 71 (2005) 031914, http://dx.doi.org/10.1103/PhysRevE.71.031914.

[49] R.A. Böckmann, B.L. de Groot, S. Kakorin, E. Neumann, H. Grubmüller, Kinetics, statistics, and energetics of lipid membrane electroporation studied by molecular dynamics simulations, Biophys. J. 95 (2008) 1837–1850, http://dx.doi.org/10.1529/biophysj.108.129437.

[50] M.J. Ziegler, P.T. Vernier, Interface water dynamics and porating electric fields for phospholipid bilayers, J. Phys. Chem. B 112 (2008) 13588–13596, http://dx.doi.org/10.1021/jp8027726.

[51] Z.A. Levine, P.T. Vernier, Life cycle of an electropore: field-dependent and field-independent steps in pore creation and annihilation, J. Membr. Biol. 236 (2010) 27–36, http://dx.doi.org/10.1007/s00232-010-9277-y.

[52] M.L. Fernández, M. Risk, R. Reigada, P.T. Vernier, Size-controlled nanopores in lipid membranes with stabilizing electric fields, Biochem. Biophys. Res. Commun. 423 (2012) 325–330, http://dx.doi.org/10.1016/j.bbrc.2012.05.122.

[53] M.-C. Ho, M. Casciola, Z.A. Levine, P.T. Vernier, Molecular dynamics simulations of ion conductance in field-stabilized nanoscale lipid electropores, J. Phys. Chem. B 117 (2013) 11633–11640, http://dx.doi.org/10.1021/jp401722g.

[54] J.N. Sachs, P.S. Crozier, T.B. Woolf, Atomistic simulations of biologically realistic transmembrane potential gradients, J. Chem. Phys. 121 (2004) 10847–10851, http://dx.doi.org/10.1063/1.1826056.

[55] A.A. Gurtovenko, I. Vattulainen, Pore formation coupled to ion transport through lipid membranes as induced by transmembrane ionic charge imbalance: atomistic molecular dynamics study, J. Am. Chem. Soc. 127 (2005) 17570–17571, http://dx.doi.org/10.1021/ja053129n.

[56] S.K. Kandasamy, R.G. Larson, Cation and anion transport through hydrophilic pores in lipid bilayers, J. Chem. Phys. 125 (2006) 074901, http://dx.doi.org/10.1063/1.2217737.

[57] L. Delemotte, F. Dehez, W. Treptow, M. Tarek, Modeling membranes under a transmembrane potential, J. Phys. Chem. B 112 (2008) 5547–5550, http://dx.doi.org/10.1021/jp710846y.

[58] L. Delemotte, M. Tarek, Molecular dynamics simulations of lipid membrane electroporation, J. Membr. Biol. 245 (2012) 531–543, http://dx.doi.org/10.1007/s00232-012-9434-6.

[59] C. Kutzner, H. Grubmüller, B.L. de Groot, U. Zachariae, Computational electrophysiology: the molecular dynamics of ion channel permeation and selectivity in atomistic detail, Biophys. J. 101 (2011) 809–817, http://dx.doi.org/10.1016/j.bpj.2011.06.010.

[60] A. Polak, M. Tarek, M. Tomšič, J. Valant, N.P. Ulrih, A. Jamnik, et al., Electroporation of archaeal lipid membranes using MD simulations, Bioelectrochemistry 100 (2014) 18–26, http://dx.doi.org/10.1016/j.bioelechem.2013.12.006.

[61] M. Casciola, D. Bonhenry, M. Liberti, F. Apollonio, M. Tarek, A molecular dynamic study of cholesterol rich lipid membranes: comparison of electroporation protocols, Bioelectrochemistry 100 (2014) 11–17, http://dx.doi.org/10.1016/j.bioelechem.2014.03.009.

[62] F. Dehez, L. Delemotte, P. Kramar, D. Miklavčič, M. Tarek, Evidence of conducting hydrophobic nanopores across membranes in response to an electric field, J. Phys. Chem. C 118 (2014) 6752–6757, http://dx.doi.org/10.1021/jp4114865.

[63] J.B. Klauda, R.M. Venable, J.A. Freites, J.W. O'Connor, D.J. Tobias, C. Mondragon-Ramirez, et al., Update of the CHARMM all-atom additive force field for lipids:

validation on six lipid types, J. Phys. Chem. B 114 (2010) 7830–7843, http://dx.doi.org/10.1021/jp101759q.

[64] W.L. Jorgensen, J. Chandrasekhar, J.D. Madura, R.W. Impey, M.L. Klein, Comparison of simple potential functions for simulating liquid water, J. Chem. Phys. 79 (1983) 926–935, http://dx.doi.org/10.1063/1.445869.

[65] B. Hess, C. Kutzner, D. van der Spoel, E. Lindahl, GROMACS 4: algorithms for highly efficient, load-balanced, and scalable molecular simulation, J. Chem. Theory Comput. 4 (2008) 435–447, http://dx.doi.org/10.1021/ct700301q.

[66] N. Kučerka, S. Tristram-Nagle, J.F. Nagle, Structure of fully hydrated fluid phase lipid bilayers with monounsaturated chains, J. Membr. Biol. 208 (2006) 193–202, http://dx.doi.org/10.1007/s00232-005-7006-8.

[67] J.N. Israelachvili, Intermolecular and Surface Forces: Revised Third Edition, Academic Press, 2011.

[68] T.J. Lewis, A model for bilayer membrane electroporation based on resultant electromechanical stress, IEEE Trans. Dielectr. Electr. Insul. 10 (2003) 769–777, http://dx.doi.org/10.1109/TDEI.2003.1237326.

[69] O.S. Smart, J.G. Neduvelil, X. Wang, B.A. Wallace, M.S.P. Sansom, HOLE: a program for the analysis of the pore dimensions of ion channel structural models, J. Mol. Graph. 14 (1996) 354–360, http://dx.doi.org/10.1016/S0263-7855(97)00009-X.

[70] N. Castillo, L. Monticelli, J. Barnoud, D.P. Tieleman, Free energy of WALP23 dimer association in DMPC, DPPC, and DOPC bilayers, Chem. Phys. Lipids 169 (2013) 95–105, http://dx.doi.org/10.1016/j.chemphyslip.2013.02.001.

[71] T.V. Tolpekina, W.K. den Otter, W.J. Briels, Nucleation free energy of pore formation in an amphiphilic bilayer studied by molecular dynamics simulations, J. Chem. Phys. 121 (2004) 12060–12066, http://dx.doi.org/10.1063/1.1815296.

[72] V.F. Pastushenko, Y.A. Chizmadzhev, Stabilization of conducting pores in BLM by electric current, Gen. Physiol. Biophys. 1 (1982) 43–52.

[73] J.C. Neu, W. Krassowska, Asymptotic model of electroporation, Phys. Rev. E 59 (1999) 3471–3482, http://dx.doi.org/10.1103/PhysRevE.59.3471.

[74] K.C. Smith, R.S. Son, T.R. Gowrishankar, J.C. Weaver, Emergence of a large pore subpopulation during electroporating pulses, Bioelectrochemistry 100 (2014) 3–10, http://dx.doi.org/10.1016/j.bioelechem.2013.10.009.

[75] A.A. Gurtovenko, I. Vattulainen, Ion leakage through transient water pores in protein-free lipid membranes driven by transmembrane ionic charge imbalance, Biophys. J. 92 (2007) 1878–1890, http://dx.doi.org/10.1529/biophysj.106.094797.

[76] J. Dzubiella, R.J. Allen, J.-P. Hansen, Electric field-controlled water permeation coupled to ion transport through a nanopore, J. Chem. Phys. 120 (2004) 5001–5004, http://dx.doi.org/10.1063/1.1665656.

[77] J. Dzubiella, J.-P. Hansen, Electric-field-controlled water and ion permeation of a hydrophobic nanopore, J. Chem. Phys. 122 (2005) 234706, http://dx.doi.org/10.1063/1.1927514.

Maura Casciola was born in Rome, Italy, in 1986. She received the Laurea degree (cum laude) in biomedical engineering from the University of Rome "La Sapienza," Rome, Italy, in 2012. From October 2011 to March 2012, she was an Intern for the Master's Thesis in the Department of Electrical Engineering Department, University of Southern California. Her research, as a PhD student of "La Sapienza" and of the University of Lorraine, is currently concentrating on the effects of short and ultra short, high-intensity electric fields on biological systems, and the electromagnetic characterization of nanopulse microchambers.

Marina A. Kasimova was born in Moscow, Russia, in 1989. She received her master degree in biophysics at Lomonosov Moscow State University, Russia, in 2011, and her PhD degree in chemistry at the University of Lorraine, France, in 2014. Right after receiving her PhD, she joined the group of Mike Klein at Temple University in Philadelphia, USA, where she is currently working. Her research focuses on the modulation of ion channels by lipids of the plasma membrane and external factors such as electric fields.

Lea Rems was born in Novo mesto, Slovenia, in 1988. She received a B.S. degree in electrical engineering from the University of Ljubljana, Slovenia, in 2012. She is currently working towards a Ph.D at the same university, with part of the work being conducted at the University of Lorraine, France. Her main research interests include combining theoretical and experimental analyses of biological processes, in particular cell membrane electroporation, by applying methods such as numerical modeling, molecular dynamics simulations, and in vitro experiments.

Sara Zullino born in Italy, 1985. She received the Master's Degree in Biomedical Engineering from Sapienza University of Rome, Italy, in 2013. From May 2013 to September 2013, she joined as a Master's Degree Trainee the Théorie Simulations et Modélisation group of the University of Lorraine, in Nancy, France. From April 2014 to October 2014, she obtained a fellowship at INRiM — National Institute of Metrological Research, in Turin, Italy. Her current research interest, as a Ph.D. candidate of the University of Turin, is focused on the characterization of nanobubbles and nanodroplets as drug delivery systems and ultrasound contrast agents.

Francesca Apollonio (M'06) was born in Rome, Italy, in 1968. She received the Laurea degree (cum laude) in electronic engineering and Doctorate degree from the University of Rome "La Sapienza," Rome, Italy, in 1994 and 1998, respectively. In 2000, she became an Assistant Professor of the same University. Since 2012 she has been a member of the BEMS board. Her research interests include the interaction of EM fields with biological systems using both theoretical and experimental approaches. In particular, she is involved in molecular dynamic studies, modeling mechanisms of interaction, dosimetry techniques, and design of exposure systems.

Mounir Tarek born in Rabat-Morocco. He received a Ph.D. in Physics from the University of Paris in 1994. He is a Research Director in the CNRS. He joined the CNRS after a four-year tenure at the National Institute of Standards and Technology (MD USA) following three year tenure at the University of Pennsylvania (M.L. Klein group). For the last few years, he worked on large-scale state-of-the-art molecular simulations of lipid membranes and TM proteins probing their structure and dynamics. His group is a member of the Europeen Associated Laboratory EBAM **"Pulsed Electric Fields Applications in Biology and Medicine"**.